

Simulation of surface morphology and defects in heteroepitaxied thin films

M. Sahlaoui^{1,2,a}, A. Ayadi¹, N. Fazouan³, M. Addou³, M. Djafari Rouhani^{4,5}, and D. Estève⁵

¹ LPMC, Département de Physique, Faculté des Sciences, Université Chouaïb Doukkali, BP 20, El jadida, Morocco

² LPC, Département de Physique, Faculté des Sciences et Techniques, BP 523, Béni Mellal, Morocco

³ Département de Physique, Faculté des Sciences, Université ibn Tofl, Kénitra, Morocco

⁴ Laboratoire de Physique des Solides, Université Paul Sabatier, 118 route de Narbonne, 31062 Toulouse Cedex, France

⁵ LAAS, CNRS, 7 avenue Colonel Roche, 31077 Toulouse Cedex, France

Received: 7 February 2000 / Revised and Accepted: 17 November 2000

Abstract. We have performed atomic scale simulations of heteroepitaxial growth of thin films using the valence force field approximation and Monte Carlo techniques. The case of CdTe/(001)GaAs is considered. Our simulations indicate valley formation presenting (111) facets with unstable bottoms in the early stages of the growth. This roughening is a source of dislocation, as it appears to relax the elastic energy of the deposited layers by formation of V-grooves. We have used a calculated RHEED as an *in situ* control of deposited layers. Finally, we present the influence of an imperfect surface in the morphology of the deposited films.

PACS. 68.35.Ct Interface structure and roughness – 68.35.Fx Diffusion, interface formation – 61.72.Bb Theories and models of crystal defects

1 Introduction

Heteroepitaxial growth of semiconductors has increasingly been studied for many years. The main reason being the technological importance of these structures in the optoelectronics field. An interesting example is CdTe/(001)GaAs. This system with a large mismatch (14.6%) is characterized by dislocation formation at the interface [1]. These defects can be detrimental to the electrical properties of devices by acting as electron-hole recombination centers or causing problems in subsequent processing steps such as lithography [2].

Atomic scale simulation has proved useful in the understanding of strain and stress effects during growth and the description of defect nucleation mechanisms. Two approaches have been employed during last years for large systems. The static approach is the first one. The geometry of defect is defined first, then strain and stress field are calculated using theory of elasticity combined to finite element method [3,4]. Another method is to use an atomic approach with an appropriate physical model like the valence force field, or ab-initio calculations [5]. The main problems of these calculations still remain a detailed description of the elementary mechanism involved in the creation of heterostructures or defects during the epitaxial growth.

The dynamical study of elementary atomic process invoked during growth is the second way to investigate the

subject. Molecular dynamics simulation is used within a potential energy [6]. Nevertheless, this approach suffers some restriction, because of the computational limitations, and calculations are generally made in a two-dimensional lattice.

A completely different and useful method for the study of atomic details in epitaxial growth is the kinetic Monte Carlo (KMC) method. The idea of this method is to find a significant set of events in order to describe correctly the general behavior of the layer growth, and to define a realistic activation energy for each of the possible events on the surface. Using a sophisticated model, strain and stress are introduced in the activation barriers [7–9]. As a consequence, relaxation of crystal becomes necessary at each step needed to perform the growth. This type of method carry out an important computational time leading to simplify the energetic model and/or to work in a two-dimensional [7] or quasi-two-dimensional space [10].

In all above models, the point and extended defects are inherently absent. This is due to the basic principle of the solid on solid (SOS) method which excludes vacancies from the beginning. Our model goes beyond this approximation.

Our simulation procedure allows for the defect observation by taking the local strain and stress into account, using an atomic approach with a semi-empirical potential energy term. Our choice is the valence force field (VFF) which is governed by its simplicity and ability to describe semiconductor properties [11].

^a e-mail: sahlaoui@fstbm.ac.ma

The purpose of this paper is to show by Monte Carlo simulation and Valence Force Field (VFF) approximation of strain energy that grooves with (111) facets are formed as a result of the stress in the deposited layer associated with the lattice mismatch. The filling of these grooves is effected by deposition of atoms on (111) facets. The growth on an imperfect substrate is investigated. In Section 2 we describe the model and the simulation procedure. Results of the simulation are presented in Section 3.

2 Model description

The general simulation based on SOS model has previously been described in detail [12]. Our new description of the model goes beyond the SOS approximation.

A Monte Carlo (MC) process is combined with a valence force field (VFF) energetic model, in order to describe strain effects, due to different nature of material deposited on the substrate. The KMC method is based on a set of elementary atomic mechanisms. Their determination is certainly one of the key points of KMC simulation, as a significant set of events is necessary to describe the correct behavior of film growth. When an event is realized, local strain and stress fields are modified, so that the surface structure is relaxed by minimizing its strain energy, which is expressed by the VFF potential. Activation energy and a hopping rate are then calculated for each possible event on the surface. As a result, the more strained regions correspond to the lower activation energies for events. A MC time can be determined including a random part, and the event associated with the lowest time is executed. A new cycle can then begin.

Different events are involved in this simulation. We have classified them in three main categories.

(i) The classical standard events are the basic events used in most MC simulation. They are deposition, evaporation and surface migrations.

(ii) Interlayer migrations *via* interstitials are also classical events. These events permit atomic migrations from an initial position in a layer number N to a final position in a layer $N + 2$ or $N - 2$, two atomic layers above or below [13,14]. The origin of such migrations is related to the local configuration. In some circumstances a stressed atom cannot move in the layer in which is situated. Normally, the moving atom would occupy a vacant site in the layer $N + 1$ or $N - 1$. However, in the zincblende lattice, this position is an interstitial site and therefore unstable. The atom will thus move rapidly to the nearest substitutional site in layers $N + 2$ or $N - 2$. To allow the motion, the intermediary layer $N + 1$ or $N - 1$ should be fully complete, at least locally. It should be noticed that interstitial atoms are not bulk atoms, but atoms at the surface, therefore very mobile, and which correspond to interstitial configurations in the crystal. A high strain energy is associated with these configurations because of the important bond bending, thus the associated motion is several orders of magnitude faster than other types of movements.

To describe this motion, let us consider the step crossing (Fig. 1) of an atom initially in position (1) close to

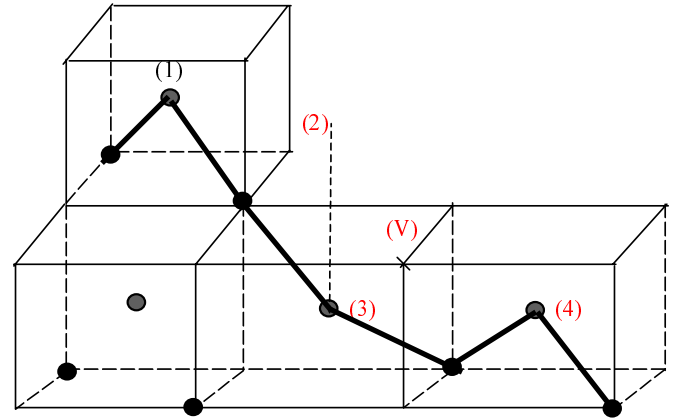


Fig. 1. Schematic representation of an interlayer migration, (1) is the initial position, (2) is a perfect crystal site where an atom cannot be fixed as the site labeled (V) is vacant, (3) is an intermediate interstitial position and (4) is the final position two layers below (1).

step edge. From site (1) the atom makes a classical migration to position (2) where it can not be fixed as the site labeled (V) is a vacant site. Consequently, the position (3) is reached as interstitial unstable position because of its bending VFF term becoming large, and thus a rapid migration leading to position (4) is executed. These motions are, of course, completely reversible. This event could be considered as a single motion, but if one decomposes it, the interstitial position stands out as a very simple and logical stage. But the outstanding point of this interlayer migration is its generalization to more than two layer crossing steps by keeping the same initial (1)-(3) and final (3)-(4) motions by introducing several intermediate interstitial-interstitial (3)-(3) motions.

(iii) Reactions between interstitial atoms are a recent improvement in our model. The reactions allow collective incorporation of atoms in interstitial positions. The result is the introduction of atoms in hanging positions (or suspended configurations) with only one bond directed toward the substrate and a second one with an atom in an upper layer as shown in Figure 2. This atomic position is of first importance for the observation of defects like vacancies or dislocations. This configuration is beyond the SOS model for semiconductors where atoms are bonded two times with the underneath layers. The SOS model excludes vacancies and overhangs from the beginning.

On the other hand, when an event is produced the structure will be relaxed. We use the VFF semi-empirical potential in order to describe the elastic part of the total energy. In our energetic model, the strain energy is expressed quadratically in terms of bond length and bond angle variations as [11,15]:

$$E_{\text{stress}} = \sum_{\text{bonds}} k_r (\Delta r / r)^2 + \sum_{\text{bond angles}} k_\theta (\Delta \theta)^2. \quad (1)$$

The force parameters k_r and k_θ are calculated from the elastic constant [11] of the materials so that no adjustable parameter is used in our simulation. In virtue of the fact

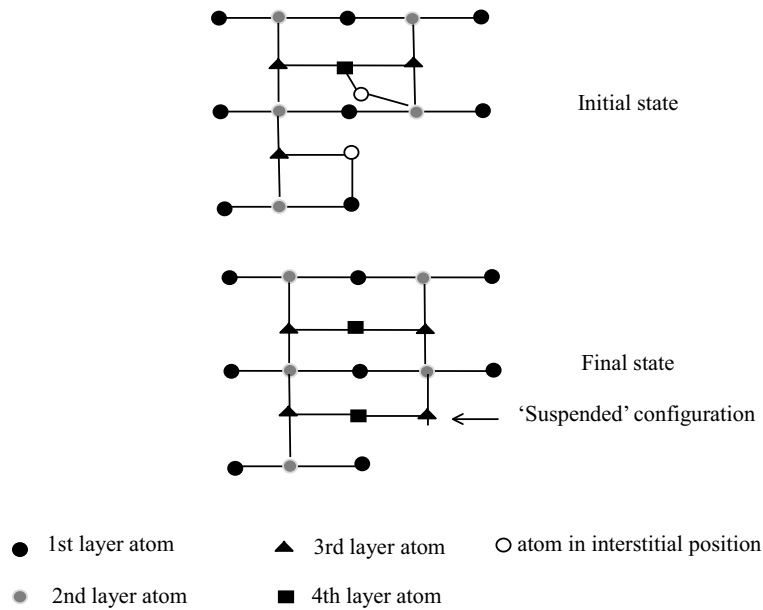


Fig. 2. Schematic representation of a reaction between interstitials giving rise to an atom in “suspended” configuration, also called “hanging” position.

that in usual semiconductors, the value of k_r is 20 to 50 times larger than k_θ , we have performed the relaxation in two steps, relaxing successively bond lengths and bond angles. We have made a further approximation in writing the energy as a quadratic expression of the atomic displacements. The analytical expression obtained is more complicated, owing to the introduction of cross-terms, but speeds up the computation, since the atomic displacements are obtained directly, using a non-iterative Newton-Raphson method.

It should be pointed out that the energy minimization is performed to adjust atomic positions around their lattice position. The atomic configurations and their bonding state are not allowed to change during this minimization. Therefore the minimization procedure leads to a local secondary minima, in agreement with the irreversible nature of the growth and the fact that the growing film should stay in a metastable state.

This VFF presents several advantages: (i) it is well adapted to non compact semiconductor structures, (ii) this model is simple enough to execute the multi-million minimizations needed to simulate the growth, (iii) activation energy is depending on the local strain can be simply defined.

3 Results and discussion

3.1 Perfect surface

Simulations of heteroepitaxial growth of thin films on an (100)-oriented substrate have been carried out and the interface structure investigated. The substrate surface was assumed to be perfect and unreconstructed. A lattice mismatch of 14.6% and physical parameters corresponding to

the case of CdTe/GaAs, were used. Typical square substrate sizes were (20×20) or (30×30) atoms. The deposition rate was fixed to 2 monolayers (ML) per second at the growth temperature of 700 K. Values of force parameter (k_θ) are set to 1.1 eV for GaAs and 0.4 eV for CdTe obtained from their elastic constants [11]. The chemical bond energy are set to 1.8 eV for GaAs and 1.0 eV for CdTe. The chemical bond energy between the substrate atom and a deposited atom is taken as 1.4 eV, the average of the bond energies of bulk GaAs and CdTe.

We have presented in a previous work [12] the consequences of interlayer migrations for CdTe/GaAs materials and their role on the layer roughening has been demonstrated. They are at the origin of the creation of valleys with (111) oriented facets along [110] and [1,-1,0] directions, in agreement with experimental observations. The deposited films are not flat, but present grooves with identical facets, in agreement with experimental observations [16–19]. When the interactions between atoms in interstitial sites are taken into account, growth is affected. A non flat surface is developed which is the sign that interlayer migrations have begun to reduce the elastic energy of the deposited film. Roughening is then introduced by (111) oriented facets (Fig. 3). The facetting is known to be due to the anisotropy of migration rate on crystallographic faces. This phenomenon allows a lateral stress relaxation of the film, the valleys bottoms are stress concentration areas where the dislocation energy barrier was calculated to be very small [26]. Atoms arriving in these valleys reach highly strained unstable positions. The energy distribution, calculated in our model in the case of Figure 3, indicates a lower energy of atoms on the surface from 0 to 0.05 eV. This results from the easy relaxation of surface atoms while bulk atoms, with three or four bound are less easily relaxed and present higher strain energy from 0.05

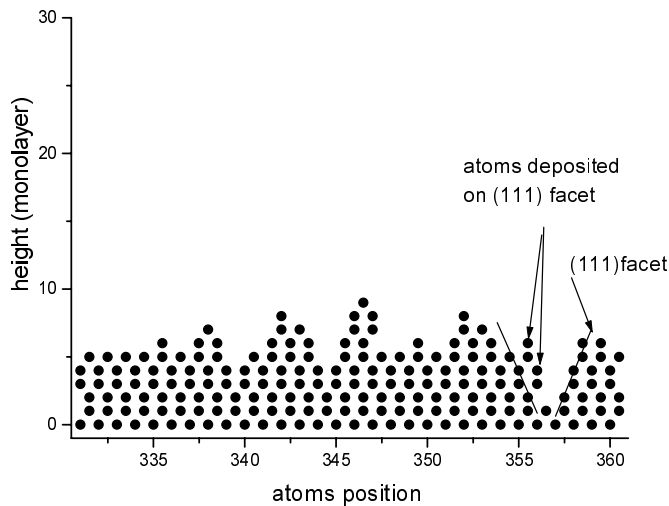


Fig. 3. Projection on a $(01\bar{1})$ plane of a growing film on a perfect surface showing V-shaped defects with (111) facets.

to 0.25 eV. But these bulk atoms are blocked by atoms in upper layers and can not move without producing cracks in the deposited film. Nevertheless the nucleation of dislocation is the combination of the atomic strain relaxation and a set of particular event that we are going to describe in what follows. As a result, an atom coming in the bottom of the valley is quasi-immediately evacuated on the (111) facets to an intermediate interstitial position with a global reduction of the elastic energy in this region. As clearly shown in Figure 3, the growth continues on (111) facets to fill the groove. In fact the mobility of atoms in interstitial sites caused by the local stress and the impossibility for these atoms to be fixed in more stable substitutional sites induce the movements of interstitial sites and lead to the growth on (111) facets. This begins with the apparition of atoms in “suspended configuration” that present a dangling bond toward the substrate and never occupy the vacancies in lower levels because of the large strain energy associated with them, but they are localized on (111) planes. The growth continues normally on the upper layers. The result is the filling of cavities by the deposition of (111) successive planes on the (111) facets, leaving vacant sites in the bottom of the grooves. This morphology can be explained in the following map. During migration and because of a significant number of atoms in interstitial positions, an atom can approach others atoms in the same situation with relative ease. The atoms can interact with each other through a common bond. These atoms which are doubly bonded are in “suspended configurations”, *i.e.* with one dangling bond towards lower layers.

Figure 3 also shows a local growth on the (111) facets. We can also observe the formation of vacancies that represent point defects within the material [20]. In fact, atoms in suspended configurations fill the cavities delimited by (111) facets and valleys in (110) directions with dangling bond toward vacant sites of the lower layers. A vacant site becomes a vacancy if it is stabilized. In fact, vacant positions may be occupied by atoms from the gaseous phase or by migrations of atoms in the deposited layers. But if

atoms are stressed at these vacant positions, they climb in the other positions to form a stable vacancy. Long term stabilization occurs when triply bonded atoms surround the vacant site.

In the first interpretation, these vacant sites are assimilated to isolated vacancies. In reality, the observation of different cross-section on successive (110) planes shows that vacancies are not isolated but grouped in lines or planes. These vacancies have a tendency to extend with growth time. They allow relaxation of the local stress and serve as a germ for interface dislocations always in very small numbers, and small sizes in the simulations.

The relaxation of the deposited layers by the formation of isolated vacancies is not an efficient process; the majority of point defects created are grouped as the defect extends. Only a few isolated point defects can be observed within the material. The extension of defects also remains limited owing to simulation conditions. Indeed, atoms in interstitial positions are very mobile and migrate between valleys formed by (111) facets. These movements are indispensable for the creation of defects, but considerably increase the computation time. To obtain a reasonable calculation time, we have been forced to slow more or less, the totality of movements on the surface. Thus, conditions of simulation are far from the thermodynamic equilibrium as the experimental conditions. Consequently germs of dislocations that form in different positions of the layer have not enough time, when growing, to be aligned on a long range. As a result of this slowing movements, some atoms in the bottom of valleys are covered by incoming atoms, before having time to relax. In these cases, the relaxation of strain occurs a few atomic distances away, causing a segmented dislocation line.

So, in order to study morphological structure and dynamic growth of strained CdTe film in a more quantitative way, the simulations of reflection high energy electron diffraction (RHEED) have been carried out. We have calculated RHEED intensity using kinematic theory for out-of-phase condition defined by $q_{\perp}d = \pi$, where q_{\perp} is the momentum transfer normal to the surface, and d is the step height corresponding to adjacent (100) atomic plane. Under such condition, the specular beam intensity of RHEED is inversely related to the degree of surface roughness which has calculated as the fluctuation in the height to which the film has grown in a given local region of substrate [23].

Figure 4a shows the calculated RHEED of the dynamic heteroepitaxial growth (CdTe/GaAs) and homoepitaxial growth (GaAs/GaAs) used for comparison. The figure gives informations on the growth mode. The oscillations are interpreted as a layer by layer growth for the homoepitaxy case, one period of the RHEED intensity oscillations corresponding to the completion of two monolayers. On the contrary, in heteroepitaxial growth, we can note clear oscillations during first stage of growth, after that a decrease of the RHEED intensity is observed, in agreement with experimental observation [24] (case of CdTe on ZnTe). This situation corresponds to the Stranski-Krastanov mode for CdTe/GaAs. In fact, during first

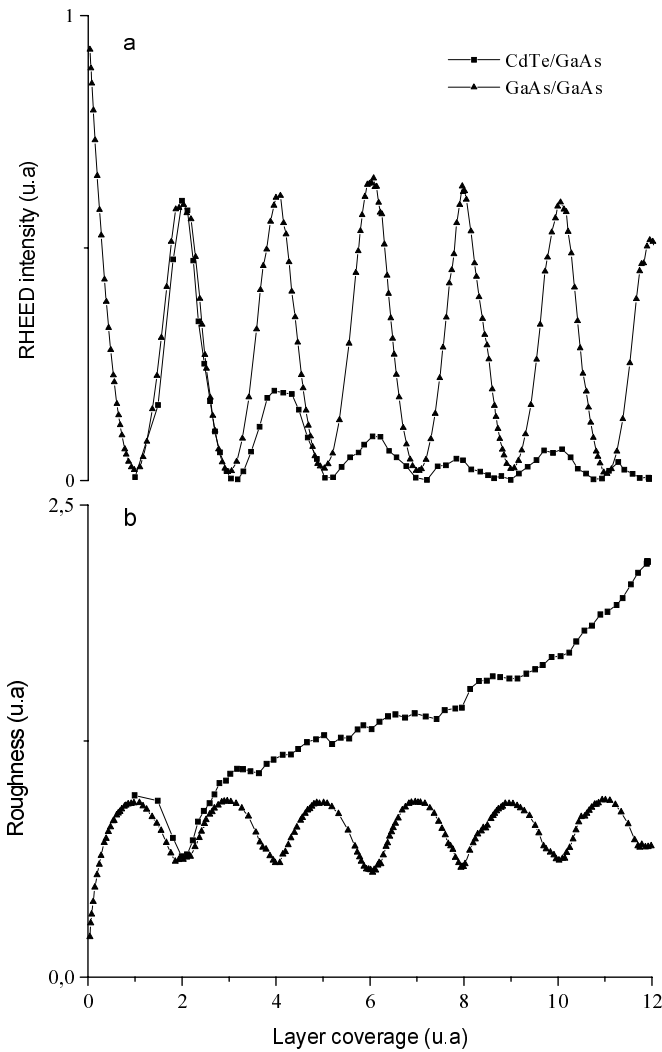


Fig. 4. (a) Rheed oscillations *versus* coverage (or time: growth rate is 2ML/s) in two cases: homoepitaxial growth (GaAs/GaAs) and heteroepitaxial growth (CdTe/GaAs). (b) The roughness of deposited layers.

stage of growth, the high-bond energy between deposited layer and substrate leads to the interlayer migrations toward a lower layer where atoms are stabilized and then allow initial layer by layer growth. This is generally the case of homoepitaxial growth where the interactions between second nearest neighbours are important [25]. We ascribe the change in the RHEED intensity to the relaxation of deposited layers and the formation of the three dimensional clusters with (111) facets as described below. The growth continues on the upper layers inducing a rough front of growth as seen in Figure 4b.

3.2 Imperfect surface

The influence of defects on the surface is an interesting problem that we have started to investigate. In this section we report preliminary results on two examples of an imperfect surface. The first case correspond to 1 ML height

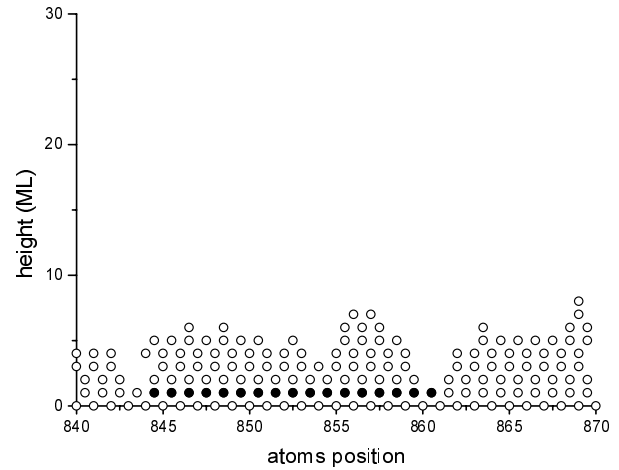


Fig. 5. Cross section of the growing film in the case of the stepped surface.

step on the substrate formed by 30×30 atoms. The planes are numbered from 1 to 30 in $[110]$ or $[1,-1,0]$ direction. In the second case, we study the effects of the presence of floating atoms from the substrate on the growth. We first start by the 1ML step case. Figure 5 shows the cross section of the growing film by a (110) plane, taken out of our simulations. Dark circles represent the step atoms. We noted firstly that the morphology in the successive (100) planes shows large variations of the statistical layer height fluctuations from one to another plane. For a better clarity we have chosen the plane number 28 represented in Figure 5. We can observe the atomic arrangement at the step edge. We can see a typical structure of the dislocation with the valley appearing at the first stage of the growth localized near the step edges. The dislocation formation mechanism is the same as described previously. The difference is that the valleys are well expanded in height and strongly localized near the step edge. This difference results from the strain and stress fields generated by the step. Consequently, a missing half plane is going to be formed at the bottom of the valley near the step edge. The global morphology of the growing films shows the presence of depressions characteristic of dislocation at the step edges [20].

In the literature, the steps have been expected to have a singular influence in the defects generation. In our simulation, we have noticed that step edges neighborhood are favorable for localization of dislocation in agreement with experimental observations [21,22].

In the second case the deposition started with some atoms from the substrate adsorbed on a (100) flat surface. These atoms are distributed randomly and cover the substrate with approximately 33% in the example represented in Figure 6. Dark circles represent these adsorbed atoms. Figure 6 shows a cross section of the deposited film. We can observe clearly that grooves are well expanded in height in comparison to the case of a perfect surface. This behavior is due to the strain and stress generated by the presence of atoms from the substrate in the first layer. In fact these atoms permit the stabilization of the

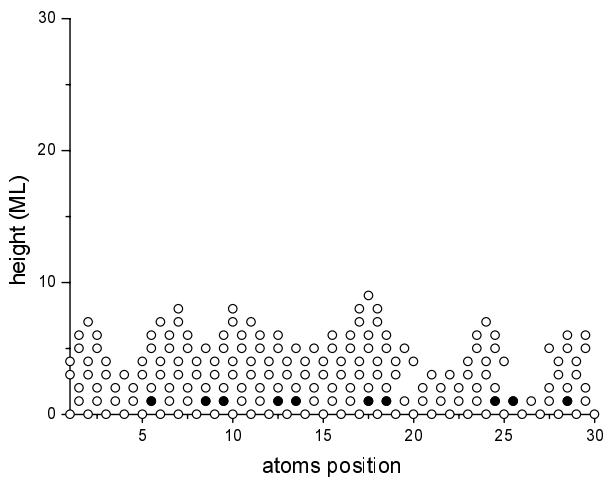


Fig. 6. Cross section of growing film in the case of a surface with floating atoms from the substrate.

substrate, but increase the stress on the upper layers. In Figure 5, we can also observe that 5 grooves are formed on a square substrate composed of 30 atoms along a [011] direction. This corresponds also to a dislocation spacing evaluated as 31 \AA which is consistent with the 14.6% of the CdTe/GaAs structure [1].

The presence of defects on substrate surface modifies strongly the film morphology, strain relief, and defect structure. As a perspective, we speculate to use an appropriate surfactant on the surface to relieve lattice mismatch and to exclude defects from the active regions.

4 Conclusion

In this article, we have described an atomic defect nucleation mechanism by associating the Monte Carlo technique and the VFF model for the simulation of film growth. The process presented is based on three main points which are valley formation presenting (111) facets with unstable bottoms, interstitial multiplication, and reaction allowing the narrowing of valley facets to form a dislocation. We have used the kinematic theory of RHEED as an *in situ* control of deposited layers and a test for a validity of the model. On the other hand, the presence of steps or floating atoms from the substrate were

qualitatively identified to localize defects because of the important strain and stress in these regions.

References

1. F.A. Ponce, G.B. Anderson, J.M. Ballingal, Surf. Sci. **168**, 564 (1986).
2. H. Tatsuoka, H. Kuwabara, H. Fyiyasu, Y. Nakanishi, J. Appl. Phys. **65**, 2073 (1989).
3. T. Benabbas, P. François, Y. Androussi, A. Lefebvre, J. Appl. Phys. **80**, 2763 (1996).
4. W. Yu, A. Madhukar, Phys. Rev. Lett. **79**, 905 (1997).
5. R. Car, M. Parrinello, Phys. Rev. Lett. **55**, 2471 (1985).
6. L. Dong, J. Schnitker, R.W. Smith, D.J. Srolovitz, J. Appl. Phys. **83**, 217 (1998).
7. A.F. Voter, Phys. Rev. B **34**, 6819 (1986).
8. M. Schroeder, P. Smilauer, D.E. Wolf, Phys. Rev. B **55**, 10814 (1997).
9. A.L. Barabasi, Appl. Phys. Lett. **70**, 2565 (1997).
10. B.G. Orr, D. Kessler, C.W. Snyder, L. Sander, Europhys. Lett. **19**, 33 (1992).
11. R.M. Martin, Phys. Rev. B **1**, 4005 (1970).
12. M. Sahlaoui, M.Djafari Rouhani, D. Estève, A. Ayadi, Appl. Surf. Sci. **151**, 218 (1999).
13. J.W. Evans, Phys. Rev. B **43**, 3897 (1991).
14. D.R.M. Williams, M. Krishnamurthy, Appl. Phys. Lett. **62**, 1350 (1993).
15. P.N. Keating, Phys. Rev. **145**, 637 (1966).
16. G. Patriarache, J.P. Rivière, J. Castaing, J. Phys. III France **3**, 1189 (1993).
17. F.K. Le Goues, M. Copel, R.M. Tromp, Phys. Rev. B **42**, 11690 (1990).
18. S. Higuchi, Y. Nakanashi, J. Appl. Phys. **7**, 4277 (1992).
19. H. Gao, W.D. Nix, Annu. Rev. Mat. Sci. **29**, 173 (1999).
20. J. Dalla Torre, M. Djafari Rouhani, R. Malek, D. Estève, A. Rocher, J. Appl. Phys. **84**, 5487 (1998).
21. N. Otsuka, C. Choi, Y. Nakamura, S. Nagakura, R. Fisher, C.K. Peng, H. Morkoç, Appl. Phys. Lett. **49**, 277 (1986).
22. Y.H. Lo, M.C. Wu, H. Lee, S. Wang, Z. Liliental-Weber, Appl. Phys. Lett. **52**, 1386 (1988).
23. J.M. Van Hove, C.S. Lent, P.R. Pukite, P.I. Cohen, J. Vac. Sci. Technol. B **1**, 741 (1983).
24. J. Cibert, Y. Gobil, Le Si Dang, S. Tatarenko, Appl. Phys. Lett. **56**, 292 (1990).
25. M. Djafari Rouhani, N. Fazouan, A.M. Gué, D. Estève, Vacuum **46**, 931 (1995).
26. D.E. Jesson, S.J. Pennycook, J.M. Baribeau, D.C. Houghton, Phys. Rev. Lett. **71**, 1744 (1993).